

Metric-Based Symbol Predistortion Techniques for Peak Power Reduction in OFDM Systems

Serdar Sezginer, *Member, IEEE*, and Hikmet Sari, *Fellow, IEEE*

Abstract—In this paper, we present a novel metric-based symbol predistortion algorithm and describe three variants for peak-to-average power ratio (PAPR) reduction in OFDM transmission. The algorithm consists of predistorting a set of input symbols per block using simple metrics, which measure how much each symbol contributes to the output signal samples of large magnitudes. The symbols to be predistorted in each block are selected as those with the largest positive-valued metrics. Predistortion of input symbols is performed either by scaling only the amplitude or by scaling separately the real and/or the imaginary parts of the selected symbols. The simple metric-based structure of the proposed algorithm gives high flexibility which enables various tradeoffs between performance and complexity. Another important feature is that the algorithm does not require transmitting any side information to the receiver and it does not involve any additional complexity for symbol detection at the receiver side. It is shown by simulations that a considerable improvement can be achieved with these simple techniques, which can be implemented as one-shot or iterative procedures.

Index Terms—OFDM, peak-to-average power ratio, PAPR reduction, symbol predistortion.

I. INTRODUCTION

AFTER its adoption for digital audio broadcasting (DAB) and terrestrial digital video broadcasting (DVB-T) over a decade ago, orthogonal frequency-division multiplexing (OFDM) has recently become very popular in wireless communications. Indeed, the IEEE 802.11a specifications for wireless local area networks (LANs) and the principal mode of the IEEE 802.16 specifications for broadband wireless access at frequencies below 11 GHz are based on this technique, and OFDM also appears today as a very strong candidate for the fourth generation of mobile cellular systems.

But the flexibility and other attractive features of OFDM may be counter balanced by its high peak-to-average power ratio (PAPR), which is substantially higher than that of single-carrier transmission. Its increased PAPR requires a large back off of the transmit power amplifier from its output saturation point, and this back off leads to a very inefficient use of the available power. This problem is particularly important on the uplink, because of the stringent low-cost and power consumption requirements on user terminals.

The PAPR problem of OFDM has been studied considerably and a number of techniques have been developed to reduce

it. Possible peak power reduction techniques include coding, clipping, phase optimization, and multiple signal representation (see, e.g., [1], [2], and references therein). All of these techniques achieve PAPR reduction at some cost. Coding reduces the useful data rate, which is undesirable [3]. Clipping, which is the simplest technique, results in spectral regrowth and error performance degradation [4]. As an alternative, PAPR reduction can be achieved using phase optimization [5] or schemes relying on multiple signal representation, such as the Selected Mapping (SLM) and Partial Transmit Sequences (PTS) algorithms introduced in [6] and [7]. The main problem of these techniques is that they require the transmission of side information to the receiver. More recent attempts reduce the peak power by changing the signal constellation, introducing new constellations, or inserting pilot signals either in unused subcarriers or over some or all of the used subcarriers [1], [8]–[14].

A simple metric-based symbol predistortion algorithm to reduce OFDM peak power was recently introduced in [15] and [16], and remarkable improvements were observed for QPSK signaling. This paper presents the general principle and describes three different variants of that symbol predistortion algorithm in a more general context. The algorithm is based on predistorting a subset of each input symbol block and involves the computation of symbol metrics which give a measure of the contribution of each symbol to the output signal samples of large magnitude. Its metric-based structure and direct operation in the frequency domain make the algorithm significantly different from the previous techniques reported in [8] and [9], where the notion of symbol predistortion first appears. The parameters inherent to the structure of the proposed algorithm give a high flexibility, which enables various tradeoffs between performance and complexity. After calculating the symbol metrics, symbol predistortion can be performed on only the amplitudes of the selected symbols or on both their amplitudes and the phases. All of these possible variants can be used as a one-shot or an iterative procedure.

The rest of the paper is organized as follows. Section II gives the general definitions and fundamental concepts relating to the PAPR problem in OFDM transmission. In Section III, following a discussion on symbol predistortion, we introduce our metric-based PAPR reduction algorithm together with its three variants, namely, simple amplitude predistortion, multilevel amplitude predistortion, and complex predistortion. Section IV is devoted to parameter selection for the metrics and the performance results of these techniques for different signaling formats including QPSK, 16-QAM and 64-QAM. Finally, our conclusions and perspectives are given in Section V.

Manuscript received December 8, 2005; revised May 25, 2006, October 17, 2006, and December 4, 2006; accepted December 5, 2006. The associate editor coordinating the review of this paper and approving it for publication was A. Molisch.

S. Sezginer was with SUPELEC, Plateau de Moulon, F-91192 Gif-sur-Yvette, France. He is now with Sequans Communications, La Défense, F-92073 Paris, France (e-mail: serdar@sequans.com).

H. Sari is with the Telecommunications Department, SUPELEC, Plateau de Moulon, F-91192 Gif-sur-Yvette, France (e-mail: hikmet.sari@supelec.fr). Digital Object Identifier 10.1109/TWC.2007.05955.

II. THE PAPR PROBLEM IN OFDM

In OFDM transmission, the complex data symbol block $\mathbf{a} = [a_0, \dots, a_{N-1}]^T$ is passed to an N -point inverse fast Fourier transform (IFFT) to obtain the discrete time-domain samples to be transmitted. The transmitted signal samples can be written as

$$b_n^l = \frac{1}{\sqrt{N}} \sum_{m=0}^{N-1} a_m^l e^{j2\pi nm/N}, \quad (1)$$

where l is the OFDM symbol index and a_m^l is the data symbol transmitted over the m th subcarrier. For convenience, the symbol index will be omitted in the sequel.

The samples to be transmitted are passed through a parallel-to-serial (P/S) converter, and then a cyclic prefix (CP) is inserted. The resulting signal samples are filtered and frequency up-converted, and the RF signal is sent to a high-power amplifier (HPA) with nonlinear characteristics. The efficiency of this amplifier is directly related to the dynamic range of the input signal.

The data symbols (the a_m 's) are independent, identically distributed (i.i.d.) random variables. From the central limit theorem, the time-domain samples at the IFFT output can be modeled as truncated zero-mean Gaussian random variables for large N . Thus, the magnitudes of most output samples will be small, but a small percentage of them will take very large magnitudes [1]. This results in the well-known PAPR problem of OFDM systems. Indeed, the high PAPR of the signal decreases the efficiency of the HPA and imposes the use of costly amplifiers, which is unacceptable especially on the uplink of wireless systems. Hence, the PAPR reduction algorithms play a crucial role at the transmitter of multicarrier systems.

The PAPR of the time-domain sample sequence $\mathbf{b} = [b_0, \dots, b_{N-1}]^T$ is defined as

$$PAPR(\mathbf{b}) = \frac{\|\mathbf{b}\|_\infty^2}{E \left\{ \|\mathbf{b}\|_2^2 \right\} / N}, \quad (2)$$

where $\|\cdot\|_p$ denotes the p -norm of the enclosed vector.

In order to investigate the performance of a PAPR reduction algorithm, it is more relevant to examine the PAPR of an oversampled signal closely approximating the transmitted continuous-time signal. In this paper, this is performed by employing the IFFT of the zero-padded input data sequence of length QN , where Q denotes the oversampling rate.

In the literature, the most common way to evaluate performance is to determine the probability that the PAPR of a block is larger than a certain level γ . This is represented by the Complementary Cumulative Distribution Function (CCDF) of the $PAPR(\mathbf{b})$, which is a random variable, as

$$CCDF_{PAPR(\mathbf{b})}(\gamma) = \Pr(PAPR(\mathbf{b}) > \gamma). \quad (3)$$

The next section presents the concept of symbol predistortion and the proposed metric-based algorithm and describes its three main variants.

III. SYMBOL PREDISTORTION

Because of their interesting features in PAPR reduction, symbol predistortion techniques have recently drawn considerable attention. They mainly tend to play with the constellation intelligently and predistort the transmitted data symbol values without affecting the minimum distance (see, e.g., [8]-[11]). These methods actually increase the average power of the IFFT output which results in a slight degradation in the system bit error rate (BER) as the average power is decreased to its original value. However, since the high peaks occur with a small probability, the increase in average power will not be a problem and can be easily controlled in our proposed scheme (e.g., by limiting the number of predistorted symbols per block).

Basically, for the QPSK signal constellation, symbol predistortion can be performed by modifying the symbols such that the magnitudes of predistorted symbols are higher than the nominal symbol values. In our case, symbol predistortion is performed by a proper scaling factor $d_m > 1$, where the index m belongs to a set covering the indices of the input symbols to be predistorted (see Fig. 1(a)). This figure clearly shows that if either the in-phase or the quadrature component of the transmitted signal is decreased below its nominal value, the minimum distance will decrease. This kind of predistortion can be easily extended to higher-level M -state quadrature amplitude modulation (M -QAM) and M -state phase-shift keying (M -PSK) signal constellations in a way similar to the one discussed in [8], by limiting the predistortion to the outer points. Fig. 1(b) shows an example for the extension of this procedure to 16-QAM. Specifically, the corner points of the constellation can be expanded as in QPSK, while only the real or the imaginary parts of the side symbols can be expanded in order not to reduce the minimum distance in the signal space. Clearly, the inner points of the constellation cannot be altered without affecting the minimum distance, and therefore they are left unchanged.

Conventional algorithms based on symbol predistortion need complex optimization to obtain the right parameters minimizing the PAPR [8][10][11]. Considering the expansion process shown in Fig. 1(a), the problem of PAPR minimization for symbol predistortion can be formulated as

$$\begin{aligned} & \underset{\mathbf{d}}{\text{minimize}} && \mathcal{L} \\ & \text{subject to} && |b_n + \mathbf{f}_n \mathbf{A}(\mathbf{d} - \mathbf{1}_N)| \leq \mathcal{L} \quad \text{for } n = 0, \dots, N-1, \\ & && \text{and } \mathbf{d} \geq \mathbf{1}_N, \end{aligned} \quad (4)$$

where $\mathbf{A} = \text{diag}(a_0, \dots, a_{N-1})$, $\mathbf{d} = [d_0, \dots, d_{N-1}]^T$, $\mathbf{1}_N$ denotes the $N \times 1$ all-one vector, and \mathbf{f}_n represents the $(n+1)$ th row of the IFFT operator. Here, \mathcal{L} depicts the largest magnitude of the peak reduced IFFT output. This is a convex optimization over the intersection of quadratic constraints and the vector of scaling factors \mathbf{d} . This is nothing but a special case of a quadratically constrained quadratic program (QCQP) for which the optimum solution is generally not feasible. It can be solved using well-known constrained minimization methods such as an interior point method [17]. However, the minimization process is highly complex, especially because it may require an important number of iterations.

As a practical implementation of symbol predistortion,

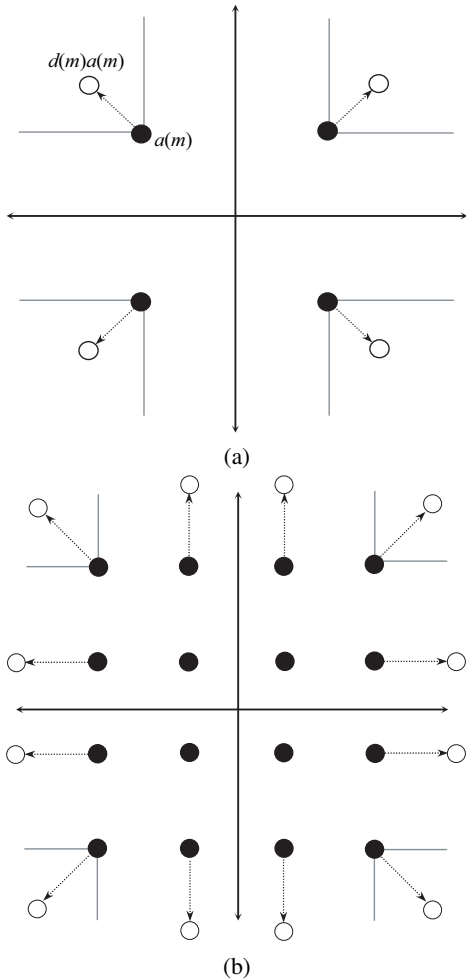


Fig. 1. Amplitude predistortion: (a) QPSK, (b) 16-QAM. Heavy dots designate nominal constellation points and hollow dots designate the corresponding predistorted points.

a technique called Projection onto Convex Sets (POCS) is described in [9]. This consists of clipping the IFFT output, taking the FFT of the clipped signal blocks, and restoring the data symbols which reduce minimum distance. This technique leads to good performance in terms of PAPR reduction, but it takes a large number of iterations to converge. For faster convergence, a gradient-based smart gradient project (SGP) method was proposed in [8]. More recently, a simple metric-based amplitude predistortion technique was introduced in [15], where the predistortion is performed using a simple scaling factor. Then, a multilevel predistortion version of this technique was introduced in [16] to further enhance performance with less average power increase. Using QPSK, it was shown that it is possible to obtain satisfactory reduction in peak power even with simple scaling of a few symbols per block.

We will now present our metric-based symbol predistortion algorithm and describe three of its possible variants, which are suboptimal solutions for the complex optimization problem. They consist of predistorting either the amplitude or both the amplitude and phase of a subset of input symbols using an appropriate metric. In the sequel, we will focus on QPSK signaling for notational simplicity. As explained above, the extension to M -QAM, for $M > 4$, is simply performed

by applying the same predistortion procedure only to the outermost constellation points.

A. Amplitude Predistortion

The proposed techniques are based on computing a metric for each input data symbol, which essentially measures how much this symbol contributes to the IFFT output samples with large values. In its general form, the metric is defined as

$$\mu_m = \frac{1}{\sqrt{N}} \sum_n w(n) f(n, m), \quad (5)$$

where $f(n, m)$ is a function which gives a convenient measure of the contribution of input symbol a_m to the IFFT output sample b_n , which is $1/\sqrt{N} a_m e^{j2\pi nm/N}$, and $w(n)$ is a weighting function of b_n . An appropriate choice for $f(n, m)$ is

$$f(n, m) = -\cos(\varphi_{nm}), \quad (6)$$

where φ_{nm} is the angle between b_n and $a_m e^{j2\pi nm/N}$. This function takes its maximum value when b_n and $a_m e^{j2\pi nm/N}$ are almost in opposite phase. In that case, symbol a_m can be predistorted to reduce the magnitude of b_n without affecting the minimum Euclidean distance, provided it belongs to the set of outer points of an M -QAM signal constellation.

The weighting function $w(n)$ is defined so as to give more weight to the output samples of large magnitude in the expression of metric μ_m . A reasonable and simple weighting function is $w(n) = |b_n|^p$, where p is an appropriately selected parameter. Using the definition $\cos(\varphi_{nm}) = \text{Re}\{b_n a_m^* e^{-j2\pi nm/N}\} / |b_n| |a_m|$, the final metric becomes¹

$$\mu_m = \frac{-1}{K\sqrt{N}|a_m|} \sum_{n \in S_K} |b_n|^{p-1} \text{Re}\{b_n a_m^* e^{-j2\pi nm/N}\}, \quad (7)$$

where K is a normalization factor and denotes the size of the set S_K whose elements are the indices of the output samples that are larger than a predetermined threshold value A . The parameter A can be taken as the value for which we obtain the greatest decrease on average PAPR. As a general rule, the value of A should be much smaller than the target PAPR value in order to take into account the possibility of the power increase of the small output samples in the metric calculation.

The metrics are computed for all input symbols of the block, and the L symbols with greatest positive metrics are determined to be predistorted with their corresponding scaling factors $d_m > 1$. For QPSK signaling, the output samples corresponding to the predistorted symbol block are next updated as

$$\bar{b}_n = b_n + \frac{1}{\sqrt{N}} \sum_{m \in S_L} (d_m - 1) a_m e^{j2\pi nm/N}, \quad (8)$$

where S_L is a set of size L whose elements are the indices of the symbols selected for predistortion in the input symbol block. Note that (8) can be easily adapted for M -QAM ($M > 4$) by limiting the summation to the outermost points and performing it separately for the corner points and the real or the imaginary parts of the side points. Given the threshold

¹In the metric proposed in [16] the normalization factor \sqrt{N} is missing. It is included here.

value A (equivalently K), the scaling factors d_m and the parameter L are determined over an exhaustive search by observing the output peak power reduction. They are ideally taken as the values after which the peak output power stops decreasing.

Again, focusing on the QPSK signal constellation, predistortion of a symbol a_m consists of transmitting $d_m a_m$, where d_m is a real number as defined above (see Fig. 1(a)). The choice of d_m and L parameters obviously has a strong impact on the performance of the proposed technique and these parameters need to be optimized. The best way to do this is to determine the parameter values leading to the lowest average peak power, the averaging being carried out over a long sequence of OFDM symbols. Although this is suboptimum compared to optimizing the parameters for every transmitted symbol block, it gives close performance results and avoids real-time optimization, thus reducing complexity.

Two variants of this amplitude predistortion are simple amplitude predistortion and multilevel amplitude predistortion.

1) *Simple Amplitude Predistortion*: Simple amplitude predistortion, as described in [15], is performed by using a constant scaling factor $d_m = \alpha$, for all $m \in S_L$, with a value greater than 1. Thus, the real and imaginary parts of the selected L input symbols to be predistorted are expanded with the same constant, which makes the implementation considerably simple. As described above, for a given value of A , we pick the parameters α and L for which we observe the largest PAPR decrease on average. The metric is evaluated as in (7) and the output samples are obtained as

$$\bar{b}_n = b_n + \frac{\alpha - 1}{\sqrt{N}} \sum_{m \in S_L} a_m e^{j2\pi nm/N}. \quad (9)$$

The procedure can be iterated one or more times using either the same or a separate $\{\alpha, L\}$ pair at each iteration.

2) *Multilevel Amplitude Predistortion*: Multilevel amplitude predistortion involves the expansion with a scaling factor d_m which differs from symbol to symbol. An intuitive solution for this expansion is to define the d_m 's as a function of the symbol metrics. For this technique, we define the expansion factor as

$$d_m = (1 + \beta \sqrt{\mu_m^+}), \quad (10)$$

where β is a positive real number. The notation $(\cdot)^+$ is used to indicate that only the positive-valued metrics are considered for symbol predistortion. The choice of the parameter pair $\{\beta, L\}$ in this technique has a strong impact on the PAPR reduction performance, and these parameters are determined as the parameter pair $\{\alpha, L\}$ in the simple amplitude predistortion described above. Finally, the output samples are updated as

$$\bar{b}_n = b_n + \frac{\beta}{\sqrt{N}} \sum_{m \in S_L} \sqrt{\mu_m^+} a_m e^{j2\pi nm/N}. \quad (11)$$

Note that the metric information is directly used in the predistortion process. Hence, for the metric definition (5), the choice of the weighting function $w(\cdot)$, the contribution function $f(\cdot)$, and as a result the optimization of the related parameter set (in our case $\{A, p\}$) appearing in (7) become more crucial. Although optimization of the metric may bring

some improvement, it seems almost impossible and it is beyond the scope of this paper.

B. Complex Symbol Predistortion

Now, we extend symbol predistortion to the phase dimension. In the complex predistortion case, the contribution of the real and imaginary parts are evaluated using separate metrics and both parts are predistorted in a fashion similar to multilevel amplitude predistortion using the two metrics. Redefining (7) separately for the real and imaginary parts of a_m , we obtain the metrics of $\text{Re}\{a_m\}$ and $\text{Im}\{a_m\}$ respectively as

$$\mu_{m,R} = \frac{-1}{K_R \sqrt{N} |\text{Re}\{a_m\}|} \sum_{n \in S_{K_R}} |b_n|^{p-1} \text{Re}\{a_m\} \times \text{Re}\{b_n e^{-j2\pi nm/N}\} \quad (12)$$

and

$$\mu_{m,I} = \frac{-1}{K_I \sqrt{N} |\text{Im}\{a_m\}|} \sum_{n \in S_{K_I}} |b_n|^{p-1} \text{Im}\{a_m\} \times \text{Im}\{b_n e^{-j2\pi nm/N}\}. \quad (13)$$

Determination of proper values for the parameters which appear in these two expressions is quite involved. Although the parameters are set beforehand, it is much more convenient to utilize the same parameters in both metrics. This is not the optimum solution, but it is reasonable because of the symmetric distribution of symbols. Further simplifications result in the following metrics:

$$\mu_{m,R} = \frac{-\text{sgn}(\text{Re}\{a_m\})}{K \sqrt{N}} \sum_{n \in S_K} |b_n|^{p-1} \text{Re}\{b_n e^{-j2\pi nm/N}\}, \quad (14)$$

$$\mu_{m,I} = \frac{-\text{sgn}(\text{Im}\{a_m\})}{K \sqrt{N}} \sum_{n \in S_K} |b_n|^{p-1} \text{Im}\{b_n e^{-j2\pi nm/N}\}. \quad (15)$$

Note that the parameters which appear in these expressions are the same as those of amplitude predistortion, and they are determined in a similar fashion. Finally, the scaling factors are defined as $d_{m,R} = (1 + \beta \sqrt{\mu_{m,R}^+})$ and $d_{m,I} = (1 + \beta \sqrt{\mu_{m,I}^+})$ respectively for $\text{Re}\{a_m\}$ and $\text{Im}\{a_m\}$, and the output samples are computed as

$$\bar{b}_n = b_n + \frac{\beta}{\sqrt{N}} \sum_{m \in S_L} \left(\sqrt{\mu_{m,R}^+} \text{Re}\{a_m\} + j \sqrt{\mu_{m,I}^+} \text{Im}\{a_m\} \right) \times e^{j2\pi nm/N}. \quad (16)$$

After complex symbol predistortion, the resulting constellation looks similar to the one obtained by the active constellation extension (ACE) method presented in [8]. But the use of metrics and the symbol-by-symbol expansion in the frequency domain make the proposed technique considerably different from the previous ACE-based methods ([8], [9]) which use clipping. The proposed technique has also a lower complexity, as explained next.

C. Complexity

As it is clear from equations (7) and (8), our algorithm involves the parameter set $\{A, p, d_m, L\}$, which makes it highly flexible. Parameter pair $\{A, p\}$ is involved in the metric calculation, while $\{d_m, L\}$ determines the expansion process. Thanks to the simple form of the metric definition, these parameters just depend on the signal constellation, IFFT size and target PAPR level. Therefore, for a given signal constellation and IFFT size, all of these parameters can be determined beforehand to achieve a target PAPR level and the desired tradeoff between complexity and performance. The only real-time operations required to implement the algorithm are the symbol metric computations and the update of the IFFT output samples given by equations (7) and (8). The computational complexity of the metric calculation step is proportional to KN . (We recall that the parameters K and N denote the number of output samples used in the metric calculation (cf. (7)) and the IFFT size, respectively.) More specifically, for QPSK, it involves at most $7KN$ real multiplications, $3KN$ additions and N divisions (which can easily be carried out using a look-up table). Next, update of the time-domain samples has a complexity that is proportional to LN , this step simply involving $5LN$ real multiplications and $(2L + 1)N$ additions.

At a first glance, the metric defined in (7) can be viewed as the projection relation of ACE-SGP method used to find the gradient step factor [8, eq (21)]. Indeed, (7) can be put in the form

$$\mu_m = \frac{-1}{K |a_m|} \text{Re}\{a_m^* c_m\}, \quad (17)$$

where $c_m \triangleq 1/\sqrt{N} \sum_{n \in S_K} |b_n|^{p-1} b_n e^{-j2\pi mn/N}$. Hence, it appears as the dual of the projection relation given in [8] leading to an implementation directly in the frequency domain. As a natural consequence of this duality, both the ACE-based methods and the proposed symbol predistortion algorithm require similar operations such as the transitions between the time and frequency domains and the storage of the modified output sample vector at each iteration. However, its frequency-domain interpretation significantly differs the proposed algorithm from ACE-based methods. On the one hand, the proposed algorithm requires an additional storage of the predistorted L symbols. On the other hand, frequency-domain metric-based implementation has two important advantages. Firstly, metric-based techniques directly use the metric information and predetermined parameters for the predistortion process, and eliminate the additional computation of a gradient step factor [8, eq (22)], which plays a critical role in the ACE-SGP method. Secondly, since predistortion is directly performed in the frequency domain, the complexity increase with Q (the value of the oversampling factor prior to the application of the algorithm) will be much smaller for the proposed techniques. This is also a result of allowing the parameter determination to an offline process and eliminating the gradient step evaluation of ACE-SGP in real-time.

Remarks

- An interesting feature of the proposed metric-based PAPR reduction techniques, which is due to their operation in the frequency domain, is that they do not lead to spectral

widening of the transmitted signal. This is a significant advantage compared to time-domain techniques, particularly in wireless systems subjected to severe spectral masks.

- In addition to the one defined in (10), other forms of scaling factors can be employed for multilevel amplitude and complex predistortion techniques, which may result in better PAPR reduction and smaller average power increase. Moreover, the metric definition can be changed and more relevant combinations of the functions may be proposed.
- The average power increase highly depends on the parameters of the algorithm and the target PAPR value. As stated at the beginning of Section III, the increase in average power can be controlled by limiting the number of predistorted symbols per block. Although the optimization of the other parameters with an upper bound on the average power increase may be performed beforehand, it is impractical.

IV. SIMULATION RESULTS

In the simulations, we used the complex baseband representation of OFDM signals, with $N = 256$ subcarriers. We applied all investigated methods when the PAPR is larger than 6 dB. Note that in PAPR calculation, the ratio of the peak power to the initial average power (before the application of the PAPR reduction algorithm) was taken into consideration. This means that we have taken into account not only the effective PAPR after predistortion, but also the increase of average signal power due to expansion of the predistorted symbols.

First, the relevant parameters are determined. Then, the performance of the proposed techniques are presented in terms of CCDF and compared with that of the ACE-SGP method [8], which is believed to be the most relevant algorithm for our comparisons. Indeed, it is generally difficult to make a fair comparison between different PAPR reduction techniques, since each method makes a different tradeoff in terms of data rate, spectral leakage, average power, and/or BER. Comparison of our algorithm with other techniques than ACE-based methods would be quite involved, since they cannot be limited to the CCDF of PAPR and require a global performance comparison including the computation of spectral leakage, data rate loss and BER degradations. For this reason, such comparisons are left out of the scope of the paper. For simplicity, we will use in the sequel the shorthand notations MB-AP1, MB-AP2 and MB-CP respectively for simple amplitude predistortion, multilevel amplitude predistortion and complex predistortion.

A. Parameter Assessment

As discussed in Section III, the parameter set $\{A, p, d_m, L\}$ plays an important role on the performance of the proposed techniques. Parameter A should be chosen to include the output samples that are likely to increase and become close to the target PAPR level after the peak reduction process. Hence, it is necessary to take the value of A well below 6 dB. On the other hand, the power factor p simply characterizes

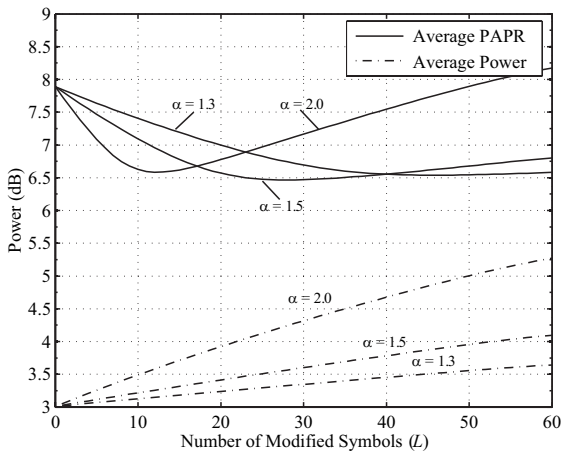


Fig. 2. Average PAPR and average power vs. number of predistorted symbols in MB-AP1 with QPSK.

the effects of the output samples' magnitudes on the metric values. Note that, the parameter pair $\{A, p\}$ highly depend on signal constellation, target PAPR level, iterations, and affect the flexibility of the algorithm. Among all, determination of these parameters need highly exhaustive search which is impractical. Hence, in our simulations, we have taken fixed values for A and p which result in satisfactory PAPR reduction with sufficiently rapid convergence. Particularly, for the MB-AP1, a threshold level A of 3.9 dB above the average power was used, and p was set to 6. The threshold level was increased to 4.7 and p was set to 5 for the techniques MB-AP2 and MB-CP.

Given the parameter pair $\{A, p\}$, the values of the pair $\{\alpha, L\}$ (resp. $\{\beta, L\}$) for MB-AP1 (resp. for MB-AP2 and MB-CP) are determined jointly through an exhaustive search so as to minimize PAPR on average using the method explained in Section III. Particularly, for MB-AP1, we have taken the step size for α as 0.01 over the interval $(1.0, 2.0]$ and observed the average PAPR for $L \in [0, 60]$. As an example, Fig. 2 shows the reduction in average PAPR as a function of the number of predistorted data symbols for three values of scaling factor α (solid-line curve) using QPSK symbols with 3 dB average power. The results are given for the first iteration and averaged over 10^6 OFDM symbols in the transmitted sequence. It also shows (dash-dotted curves) the increase of the average signal power corresponding to those values. As can be seen on this figure, the optimum number of predistorted symbols L is on the order of 10 for $\alpha = 2$ and on the order of 40 for $\alpha = 1.3$. The figure also shows that the largest PAPR reduction is achieved for $\alpha = 1.5$ and predistorting 28 data symbols, which are the optimum values obtained from the exhaustive search. For simple amplitude predistortion, these α and L values were selected for use in the first iteration, and the two parameters were separately optimized for the following iterations.

In the case of MB-AP2 and MB-CP techniques, a similar procedure was employed to obtain the optimum values for the first iteration and these values were used for all iterations. Fig. 3 shows the comparison of the average PAPR reduction between the proposed techniques for optimized α and β values again for QPSK signaling at the first iteration. For MB-AP2,

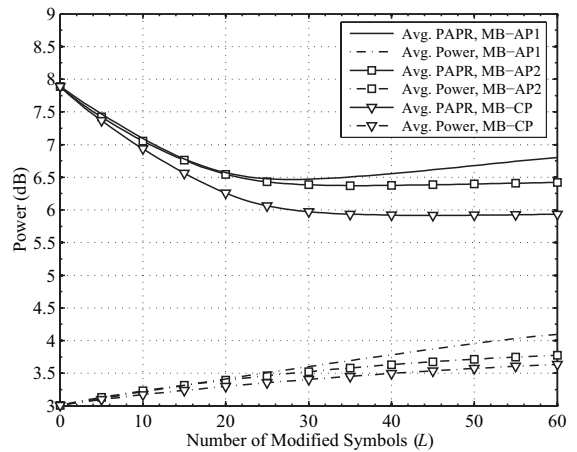


Fig. 3. Average PAPR and average power vs. number of predistorted symbols: Comparison of the proposed symbol predistortion techniques using QPSK.

the largest PAPR reduction is achieved with $\beta = 0.26$ and $L = 36$. However, MB-CP requires $L = 45$ data symbols to be modified with $\beta = 0.19$ for the best performance. It is also worth noting that as we increase the complexity slightly from MB-AP1 to MB-CP, we not only achieve a better peak power reduction but also decrease the average power increase at their first iteration. As a final remark, the PAPR reduction depicted in Figs. 2 and 3 does not reflect properly the PAPR reduction capability of the proposed techniques. They just show the change on average and give an idea for the introduced parameters. Hence, the selected parameters are far beyond the optimum ones which should be optimized separately for each OFDM block.

B. Performance Comparison

With the parameters at hand, the performances of the proposed techniques and ACE-SGP method are compared in terms of CCDF for QPSK, 16-QAM and 64-QAM signaling formats. For the proposed techniques, we kept the same values of the parameter pair $\{A, p\}$ used in the previous section. For the ACE-SGP method, the clipping value was taken as 4.86 dB above the average power (as in [8]), and this was used for all signaling formats. Throughout extensive simulations, it was observed that the performance of the proposed techniques improved with the increase in the oversampling rate Q . However, for $Q > 2$ the improvement was insignificant compared to the complexity increase. Therefore, all techniques were applied to output samples oversampled by a factor of 2, and then the oversampling factor Q was increased to 8 by interpolation at the IFFT output to approximate the analog signal. The results were obtained by averaging over 10^6 randomly generated OFDM symbols.

In Fig. 4, we present the results in terms of the CCDF for QPSK signaling. The solid-line curve in this figure corresponds to OFDM with no PAPR reduction and the marked curves correspond to the first three iterations of the proposed PAPR reduction techniques. Also, we included the first three iterations of the ACE-SGP after which no significant improvement occurs. In the case of MB-AP1, the improvement is on the order of 2 dB below the probability of 10^{-3} for the first

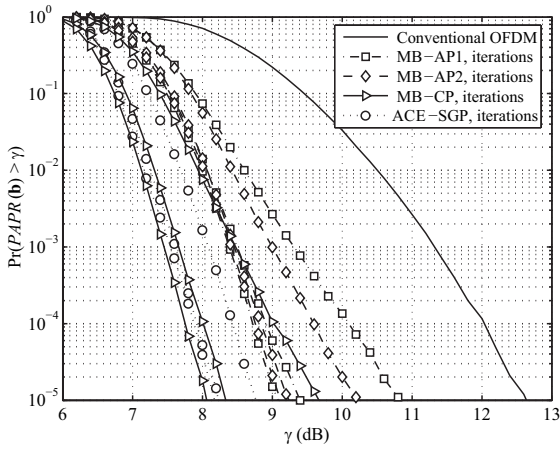


Fig. 4. CCDF of PAPR for the proposed symbol predistortion techniques and ACE-SGP using QPSK.

iteration and increases to 3 dB at the probability of 10^{-3} and to 3.5 dB at the probability of 10^{-5} at the 3rd iteration.

Compared to MB-AP1, MB-AP2 achieves at the first iteration a gain of 0.3 dB at the probability of 10^{-3} and of 0.6 dB at the probability of 10^{-5} . At the second and third iterations, however, the respective performances of the two techniques are similar. The interesting observation here is that at the second iteration, MB-CP achieves a similar convergence to the ACE-SGP method and it slightly outperforms it at the third iteration. Further iterations increase the gap between MB-CP and ACE-SGP at a cost of further increase in average power.

Next, Fig. 5 and Fig. 6 show performance results for the 16-QAM and 64-QAM signal constellations. The results are similar to those of Fig. 4. At the first iteration, MB-AP2 outperforms MB-AP1 by 0.4 dB below the probability of 10^{-3} , but the two techniques lead to similar performances at the second and third iterations. The next observation is that at the third iteration, the ACE-SGP method achieves a 0.3 dB improvement over these two techniques, and MB-CP leads to better performance at the second and third iterations below the probability of 10^{-2} . Comparing Fig. 5 and Fig. 6, we can see that the performance results corresponding to 64-QAM are very similar to those of 16-QAM. Again, the ACE-SGP method slightly outperforms MB-AP1 and MB-AP2, and MB-CP further improves performance.

The cost of the improvement in each of the techniques is the increase in average power. Table I presents the average power increase of the proposed techniques and ACE-SGP and their PAPR values at the probability of 10^{-3} at their 3rd iteration for the employed signaling formats. The average power increases of the presented techniques are close to each other especially for QPSK signaling. Although MB-CP achieves the least average power for the first iterations (which can also be inferred from Fig. 3), its slight performance improvement results in a slight average power increase compared to the other schemes at the 3rd iteration. For 16-QAM and 64-QAM, MB-AP1 gives slightly higher results than ACE-SGP. On the contrary, MB-AP2 and MB-CP achieves a smaller power increase. Note that the unstable behavior of the values for 16-QAM and 64-QAM signaling formats especially results from the restriction of the target PAPR to 6 dB which is not

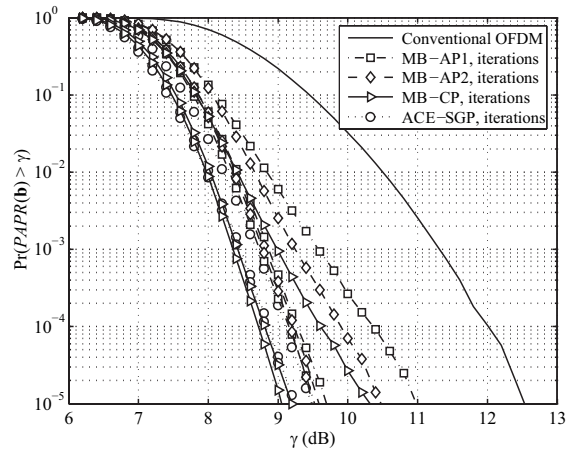


Fig. 5. CCDF of PAPR for the proposed symbol predistortion techniques and ACE-SGP using 16-QAM.

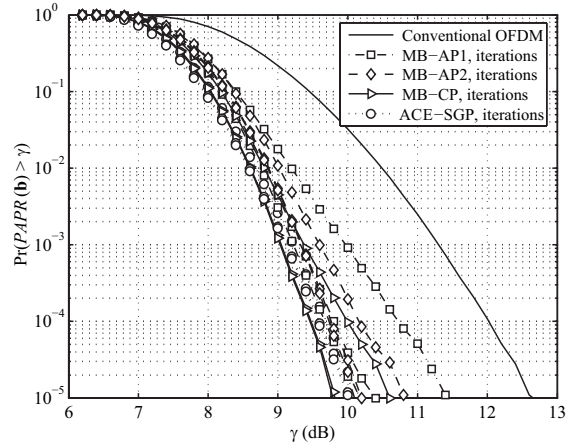


Fig. 6. CCDF of PAPR for the proposed symbol predistortion techniques and ACE-SGP using 64-QAM.

realistic in practice.

As mentioned in the previous sections, the power increase can be controlled playing with the parameters of the proposed schemes. Fig. 7 presents the CCDF of MB-CP for different values of the parameter pair $\{\beta, L\}$. First, we decrease the value of β from its optimized value 0.19 to 0.1 (dashed curves). Then, we obtain an average power increase of 0.68 dB with a slight decrease in performance. On the other hand, decreasing the number of predistorted symbols L from 45 to 20 (dashed-dotted curve) and 15 (dotted curve) provides an improvement of 0.3 and 0.4 dB respectively in terms of average power increase. In these cases, the performance degradation is on the order of 0.4 dB compared to the 3rd iteration of the optimized curve.

As a final remark, the proposed techniques share two interesting features of ACE-SGP, which are (a) performance improves with the increase in the number of subcarriers, and (b) the average power decreases when we increase the target PAPR level. The first property is due to the fact that the number of degrees of freedom increases with the number of carriers for a given percentage of predistorted symbols per block. The second property is explained by noting that the number of symbols that need to be predistorted decreases as the target PAPR is increased.

TABLE I

COMPARISON OF THE VALUE PAIR {PAPR, AVERAGE POWER INCREASE} BETWEEN THE PROPOSED TECHNIQUES AND ACE-SGP

	QPSK	16-QAM	64-QAM
MB-AP1	{8.39, 0.8782}	{8.73, 1.1322}	{9.22, 0.8888}
MB-AP2	{8.41, 0.8653}	{8.78, 0.7789}	{9.33, 0.6302}
MB-CP	{7.45, 0.9168}	{8.35, 0.8681}	{9.03, 0.7048}
ACE-SGP	{7.54, 0.8210}	{8.43, 0.9547}	{9.11, 0.8072}

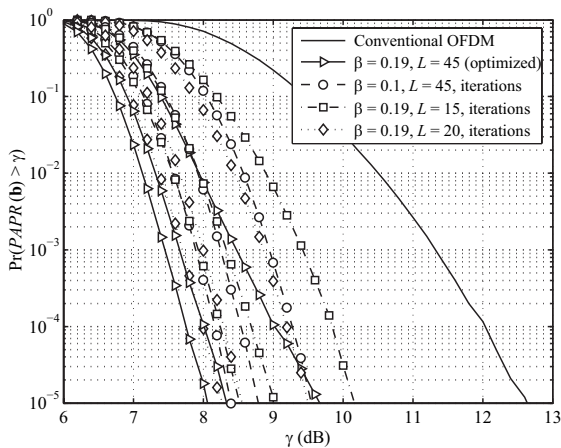


Fig. 7. CCDF of PAPR for MB-CP with different parameter values (QPSK).

V. CONCLUSIONS AND PERSPECTIVES

A metric-based symbol predistortion algorithm and three different variants have been presented. The algorithm employs an appropriately defined metric for each input symbol that measures its contribution to the output samples of large magnitude. Once the metrics are computed for all symbols of the block, a set of symbols with the largest metrics are predistorted using either simple scaling, multilevel scaling, or complex predistortion. All of these variants are very flexible, since the symbol metrics include several design parameters, and their computational complexity is low because the design parameters can be determined beforehand. The proposed techniques can be easily implemented for all M -QAM and M -PSK signaling formats, and used either as a single-shot procedure or the process can be iterated one or more times to further improve their performance. Compared to the reported results, additional improvements can be expected by jointly optimizing the parameters used in the algorithm and/or introducing other cost functions.

REFERENCES

- [1] J. Tellado, *Multicarrier Modulation with Low Peak to Average Power Applications to xDSL and Broadband Wireless*. Boston/Dordrecht/London: Kluwer Academic Publishers, 2000.
- [2] S. S. Han and J. H. Lee, "An overview of peak-to-average power ratio reduction techniques for multicarrier transmission," *IEEE Wireless Commun. Mag.*, pp. 56–65, Apr. 2005.
- [3] K. Patterson, "Generalized Reed-Muller codes and power control in OFDM modulation," *IEEE Trans. Inf. Theory*, vol. 46, pp. 104–120, Jan. 2000.
- [4] X. Li and L. J. Cimini, "Effects of clipping and filtering on the performance of OFDM," in *Proc. VTC'97*, pp. 1634–1638, May 1997.
- [5] C. Tellambura, "Phase optimization criterion for reducing peak-to-average power ratio in OFDM," *Electron. Lett.*, vol. 34, pp. 169–170, Jan. 1998.

- [6] M. Breiling, S. H. Muller, and J. B. Huber, "SLM peak-power reduction without explicit side information," *IEEE Commun. Lett.*, vol. 5, pp. 239–241, June 2001.
- [7] S. H. Muller and J. B. Huber, "OFDM with reduced peak-to-average power ratio by optimum combination of partial transmit sequences," *Electron. Lett.*, vol. 33, pp. 368–369, Feb. 1997.
- [8] B. S. Krongold and D. L. Jones, "PAR reduction in OFDM via active constellation extension," *IEEE Trans. Broadcast.*, vol. 49, pp. 258–268, Sept. 2003.
- [9] D. L. Jones, "Peak power reduction in OFDM and DMT via active channel modifications," in *Proc. 33rd Asilomar Conf. on Signals, Systems and Computers*, pp. 1076–1079, 1999.
- [10] Y. J. Kou, W.-S. Lu, and A. Antoniou, "New peak-to-average power-ratio reduction algorithms for multicarrier communications," *IEEE Trans. Circuits Syst. I*, vol. 51, pp. 1790–1800, Sept. 2004.
- [11] M. Sharif, C. Florens, M. Fazel, and B. Hassibi, "Amplitude and sign adjustment for peak-to-average-power reduction," *IEEE Trans. Commun.*, vol. 53, no. 8, pp. 1243–1247, Aug. 2005.
- [12] H. K. Kwok and D. L. Jones, "PAR reduction via constellation shaping," in *Proc. ISIT 2000*, Sorrento, Italy, June, 2000.
- [13] A. Mobasher and A. K. Khandani, "Integer-based constellation shaping method for PAPR reduction in OFDM systems," *IEEE Trans. Commun.*, vol. 54, no. 1, pp. 119–127, Jan. 2006.
- [14] B. S. Krongold and D. L. Jones, "An active set approach for OFDM PAR reduction via tone reservation," *IEEE Trans. Signal Processing*, vol. 52, no. 2, pp. 495–509, Feb. 2004.
- [15] S. Sezginer and H. Sari, "Peak power reduction in OFDM systems using dynamic constellation shaping," in *Proc. EUSIPCO'05*, Antalya, Turkey, Sept. 2005.
- [16] S. Sezginer and H. Sari, "OFDM peak power reduction using metric-based amplitude predistortion," in *Proc. GLOBECOM'05*, Saint Louis, Missouri, Nov. 2005.
- [17] S. Boyd and L. Vandenberghe, *Convex Optimization*. Cambridge University Press, 2004.



Serdar Sezginer (S'99 - M'07) was born in Bandirma, Turkey, in 1977. He received the B.Sc. and M.Sc. degrees in electrical and electronics engineering, in 2000 and 2003, respectively, both from Middle East Technical University (METU), Ankara, Turkey, and his Ph.D. degree in 2006 from University of Paris-Sud XI, Orsay, France. He is the recipient of the EEA Best Thesis Award of France in the area of signal and image processing.

He is currently with Sequans Communications, Paris, France, where he is working as a Research Engineer. His research interests mainly lie in the areas of digital communications and statistical signal processing, including synchronization, channel estimation, equalization, and diversity techniques.



Hikmet Sari (S'78 - M'81 - SM'88 - F'95) received his Diploma (M.S.) and Doctorate in Telecommunications Engineering from the ENST, Paris, France, in 1978 and 1980, respectively, and the Habilitation degree from the University of Paris-Sud, Orsay in 1992. He was with Philips Research Laboratories from 1978 to 1989, first as Researcher and then as Group Supervisor. From 1989 to 1996, he was R&D Department Manager at SAT (SAGEM Group), and from 1996 to 2000, he was Technical Director at Alcatel. In May 2000, he became Chief Scientist of the newly-founded Pacific Broadband Communications, which was acquired by Juniper Networks in December 2001. Since April 2003, he has been a Professor and Chair of the Telecommunications Department at SUPELEC, and since December 2004 he is also Chief Scientist of Sequans Communications.

Dr. Sari has published over 160 technical papers and holds over 25 patents. He was an Editor of the *IEEE Transactions on Communications* from 1987 to 1991, a Guest Editor of the *European Transactions on Telecommunications* (ETT) in 1993, a Guest Editor of the *IEEE JSAC* in 1999, an Associate Editor of the *IEEE Communications Letters* from 1999 to 2002, Chair of the Communication Theory Symposium of ICC 2002 (April 2002, New York), Technical Program Chair of ICC 2004 (June 2004, Paris), and Vice General Chair of ICC 2006 (June 2006, Istanbul). He was elevated to the IEEE Fellow Grade and received the Andre Blondel Medal from the SEE (France) in 1995 and he received the Edwin H. Armstrong Achievement Award from the IEEE Communications Society in 2003.